

An Investigation on Al6061/TiB₂ Nano Composites Production through Mechanical Alloying Route and Their Corrosion Behavior

Iman Ebrahimzadeh^{1*}, Farhad Gharavi², G.H. Borhani³

¹Advanced Materials Research Center, Department of Materials Engineering, Najafabad Branch, Islamic Azad University, Najafabad, Iran.

²Department of Materials Engineering, Sirjan Branch, Islamic Azad University, Sirjan, Iran.

³ Department of Materials Engineering, Malek-e-Ashtar University of Technology, Isfahan, Iran.

ARTICLE INFO

Article history:

Received 30 July 2017

Accepted 1 October 2018

Available online 15 September 2018

Keywords:

Al6061 nano-composite alloy

Nanocomposite

Mechanical alloying

Hot extrusion process Corrosion

ABSTRACT

Aluminum-based alloy composites with high strength and low density can be used in corrosive environments. In this research, the nano-powders of Al6061 alloy and Al6061/TiB₂ composite were synthesized by mechanical alloying (MA) method. Then, Al6061/TiB₂ nano-composite bulk samples were prepared at laboratory scale by hot extrusion approach. Transmission electron microscopy (TEM) and X-ray diffraction (XRD) devices were respectively used for measurement of particles and grains, and the polarization test was employed to assess the corrosion behavior of Al6061/TiB₂ nano-composites. The grains size of hot extrusion samples were calculated as about 95 nm. Uniform corrosion behavior and pitting of the produced nano samples of MA6061 /1.25 TiB₂ have higher corrosion resistance compared to the alloy samples of MA6061.

1-Introduction

Among various alloys of Al, 6xxx series have a wide application in various industries, in particular the constructs and aerospace industries, which is due to their acceptable strength, high weldability and corrosion resistance. The Al6061 alloy has the highest strength after T6 heat treatment, and is highly different in this regard from other alloys of this group. This alloy has a good elongation compared to other alloys of this group and can be processed as the best candidate by the MA method. Aluminum 6063 and 6061 alloys benefit from the widest area of heat treatment compared with other alloys of this group, and in such a wide range, achievement of high strength with optimal flexibility appears to be possible [1].

Using ceramic particles in the matrix of Al alloys, the researchers have attempted to

improve the modulus of elasticity and increase other properties of these alloys [2-3]. Lightweight, good mechanical properties and corrosion resistance against environment are important reasons for widely use of Al alloys with composite matrix in various industries [1]. The Al composites with whisker reinforcements or SiC particles have allocated the maximum percentage of research and development to themselves. Besides SiC, the particles of Si₃N₄, AlN, TiC, Al₂O₃ and TiB₂ have been investigated along with Al matrix [2-4]. In this regard, Narimani et al. [5] researched on Investigating the microstructure and mechanical properties of Al-TiB₂ composite fabricated by Friction Stir Processing (FSP) and they concluded that by the addition of MAed TiB₂-Al composite powder during FSP the tensile strength could increase to about 280 MPa, which was about 70% higher than that of the base

* Corresponding author:

E-mail address: i.ebrahimzadeh@pmt.iaun.ac.ir

material. Additionally, Vivekananda et.al. [6] worked on wear behavior of in situ Al/TiB₂ composite: influence of the microstructural instability, and they reported that the wear resistance of Al/5 wt% TiB₂ composite was significantly improved due to the presence of TiB₂ particle in Al matrix material. They also documented that the composite produced at melt temperature 800 °C showed a higher wear resistance at applied load: 10 N, sliding temperature: 25 °C and sliding velocity: 0.7 m/s. Moreover, Chen et. al. [7] studied on Fabrication and micro strain evolution of Al-TiB₂ composite coating by cold spray deposition, and they reported that Al-TiB₂ composite coatings (approximately 50 μm thick) were obtained retaining the microstructure of the composite powders being sprayed and no evidence of detrimental phase transformation was found. However, micro-cracks were found to exist in the Al-TiB₂ coating due to the hardly deformable powder particles. On average in the production of composites, the alloys of 6xxx and 2xxx series have had the highest rate of application as matrix [8]. The Al-SiC reaction during manufacturing operations and creation of Al₄C₃ at the intersection will be associated with reduced strength and corrosion properties. Given that, the TiB₂ cermet particles have positive indicators such as lack of reaction in the intersection with Al matrix, adequate strength at the intersection, high wear resistance and proper hardness for use in the Al matrix [8-10]. In recent years, TiB₂ particles has been synthesized as nanoparticles by using K₂TiF₆ and KBF₄ salts in the Al molten alloy [11-12]. However, the non-uniformity of TiB₂ particles distribution and

the presence of other phases as TiAl₃ and Al₂O₃ within the matrix have been always reported [12]. The ability to produce fine particles such as TiB₂ through active sintering in the matrix of the aluminum alloy has introduced this ceramic as a unique reinforcement. The corrosion resistance of Al6061 composites is greatly influenced by the presence of secondary phase [13]. The presence of secondary phase particles in the corrosion behavior of composites may increase or decrease the sensitivity to corrosion. This not only depends on the alloy composition, its microstructure and the secondary phase particles, but it is also dependent on other parameters such as the production process [14]. In a comparative study on the cathodic flow rates related to aluminum matrix composites containing SiC, Gr, TiB₂ and Al₂O₃, it was shown the density of cathodic current rate is as the order of SiC < Gr < TiB₂ < Al₂O₃ [15-16]. In this study, mechanical alloying and extrusion operation performed the laboratory production of Al6061 alloy powder and Al6061 / TiB₂ composite.

2- Materials and experiments

2-1- Raw materials

The powdered elements of aluminum, zinc, magnesium, manganese, silicon and copper were used as raw material with a purity of 99.9% (Table 1). In accordance with a the Al6061 composition, 300 g of the powder mixture along with 3 kg of steel balls were completely homogenized in the Mixer for 20 minutes (Table 2).

Table 1. Specifications of raw powders used along with their provision sources.

Powder type	Purity (%)	Particles average size (μm)
Al	99	30.90
Zn	99.99	15.00
Mn	99.99	25.00
Mg	99.9	20.00
Si	99.99	15.00
Cu	99.99	14.50
TiB ₂	99.9	2

Table 2. Al6061 chemical composition and weights of powders used in a 300 g pack.

Elements	Al	Fe	Cr	Cu	Si	Mg	Mn	Zn
Weight percentage of 6061 alloys based on Standard 1	Bal.	0.70	0.15	0.25	0.60	1.00	0.15	0.25
Weights of powdered components based on 100g samples	97.35	-	-	0.25	0.50	1.00	0.15	0.25

2-2- MA Operation

The mixture of powder and pellets were milled along with 1% stearic acid, as PCA (Process Control Agents) in an Attritor Ball Mill for 1 to 15 hours. The parameters used in the milling operation are presented in Table 3. The MA operation was conducted in two stages for the production of Al6061 / TiB₂ composite powders. In the first stage, the mixture of Al6061 powders were ground for 14.5 hrs, and subsequently, adding TiB₂ was done volumetrically by the value of 1.25-2.25%, and milling operation continued for half of an hour. The milled powders were annealed and degassed at 350 °C for 2 hrs in a vacuum atmosphere (10⁻³ Torre).

2-3- Analysis of powders

The XRF device, Philips model, tested the produced powders. The content of elements in the powdered mixture after MA operation, Fe, and Cr absorption rates were evaluated by the system. Table 4 shows the results of data from XRF testing. The TEM device, LEO-606E model, was used for accurate measurement of the size of powdered particles. The effect of MA operation on Al6061 powdered mixture and annealed powders were studied by X-ray diffraction device, model PHILIPS XD, and analysis of its crystal size was evaluated.

Table 3. Parameters used in the production of MAAl6061 nano-powder and its alloys.

Capacity (L)	Atmosphere	Rate (rpm)	Ball/Charge	Ball diameter	Container material
2.5	Argon gas	360	10	10	SS316

Table 4. XRF results of MA-Al6061 powders after 15 hours of milling operation.

Elements	Ni	Cr	Mn	Cu	Fe	Zn	Si	Mg	Al
Content (wt %)	0.028	0.030	0.250	0.290	0.490	0.250	0.70	1.20	96.64

2-4- Extrusion Operation

A value of 25 g of each sample was put inside a closed-bottom shape aluminum cylinder with a diameter of 25 mm after degassing. Followed by isolating of the cylinder in a metal mold with the same diameter of 25 mm, they were pressed under the pressure of 300 MPa [17]. The aluminum cylinder was used to protect the MA powder against oxidation during hot extrusion operation. To avoid the piece adhesion to the extrusion mold as well as reducing the pressure on the walls of the mold, the samples were impregnated with the mixture of graphite and silicon oil before extrusion. These parts were extruded with a ratio of 1: 6 after pre-heating operation at a temperature of 460 °C for Al6061 alloy and 400 °C for Al6061/TiB₂ composites.

2-5- Analysis of Components

Extruded parts were tested by XRD after surface preparation. The corrosion behavior of Al6061 alloy and its composites were investigated with use of Potentiostat/Galvanostat system (EG&G) by potentiodynamic polarization method. The solution used in this test included distilled water associated with 3.5% NaCl, which is comparable with the corrosion behavior in the marine environment [18]. In addition, the cyclic polarization test was performed on the samples to evaluate the pitting of alloys. All samples were completely grinded using 200 to 1000 emery papers and their surfaces were smoothed. The samples cross-section were circular with a diameter of 9 mm and 3 mm thickness. It should be noted that all the samples were mounted with

the help of a special gum and a soldered copper wire to the rear surface of the sample established the electrical connection with the device. Prior to perform corrosion tests, the samples surface were washed with a solution of acetone, and then, with distilled water. The sample cross-section was put in contact with the 9 mm corrosion solution. To establish the state of stability, all samples were kept for 90 minutes in a Pyrex glass vial with a volume of 300 ml. Calomel electrode as the reference electrode, a platinum electrode as the auxiliary electrode and the samples were used as working electrodes. Through immersion in solution, the samples were placed in cathodic state for 900 seconds under the potential of -1000 to -1200 mV to reduce their surface films. Anodic potentiodynamic polarization tests were performed in terms of the potential rate of 0.5 mV/s.

3- Results and Discussion

3-1- Examining produced powders

The TEM results of MA-Al6061 powders, after 15 hours of MA operation in the form of (1) show a wide range of powdered particle size. The dispersion can be calculated in the range of 20 to 70 nm. In some points, the agglomeration of powders can be seen, and such a size difference could be due to the phenomenon

occurred during prototype generation for TEM testing. Increased milling time can help to further uniformity and fining of powdered particles; although the MA operation time is very effective in increasing the contamination rate of the resulting powder, since with increased operation time, the contamination rate of powder due to contact with the container, pellets and the PCA would enhance. The final times for Al alloys vary in various mills from 30 to 130 hours. Such a drastic difference could be due to differences in milling speed, alloy system used and different pellet to powder ratios [19]. According to the results of XRD test (Fig. 2) and using the Nelson Reilly equation, the average grains size was calculated at various grinding times [20]. In addition, from Fig. 2, it is clear that all the selected picks is related to the aluminum alloy. By increasing the width of XRD spectrum due to enhanced milling time, the aluminum alloy grains size will be reduced. Fig. 3 shows the reduction in the grains size than to increased milling time for MA-Al6061 powders. The grains size has decreased to about 20 nm. Comparing Figs 1 and 3 suggests that the sizes of aluminum alloy grains and the generated particles during the process are almost identical, and in some cases because of mechanical alloying process, the particles have become so tiny that can be seen as single grains.

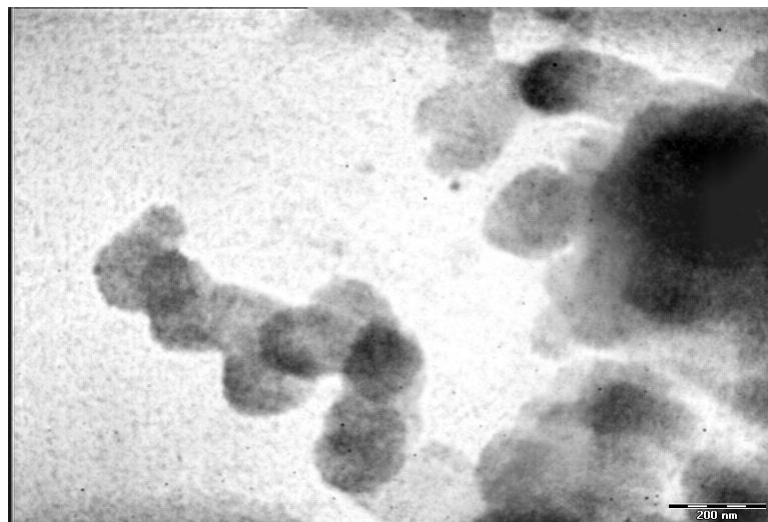


Fig. 1. The size of Al6061 powdered particles after 15 hours of milling by using TEM.

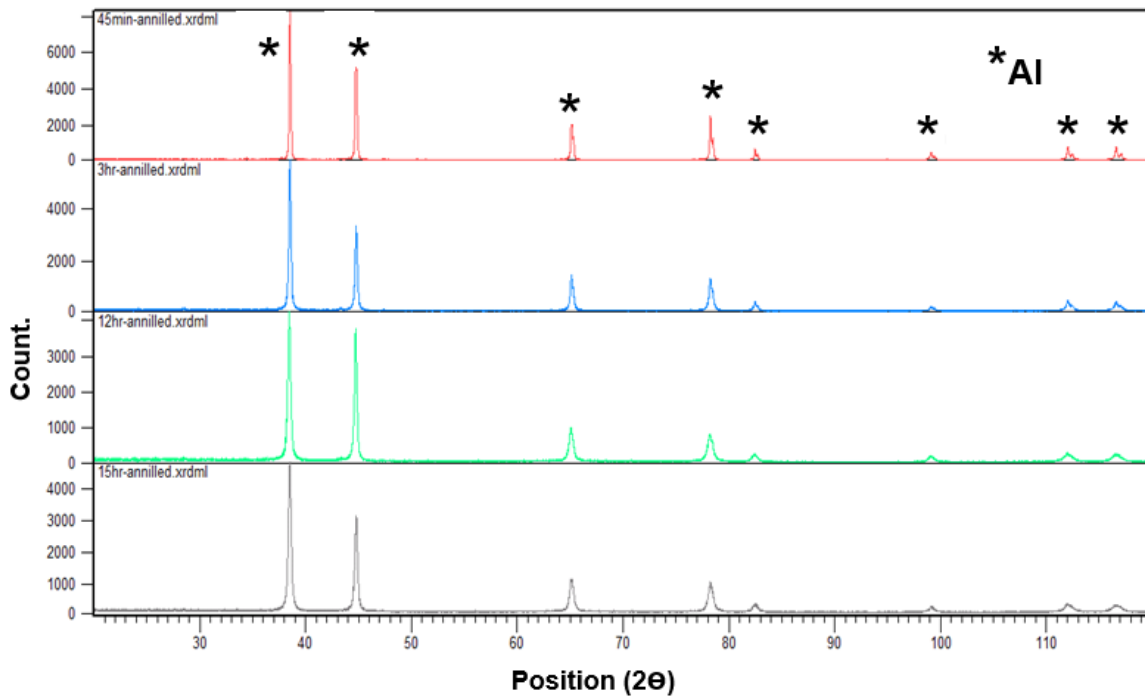


Fig. 2. Changes in the XRD peaks of Al6061 powder after annealing per milling time.

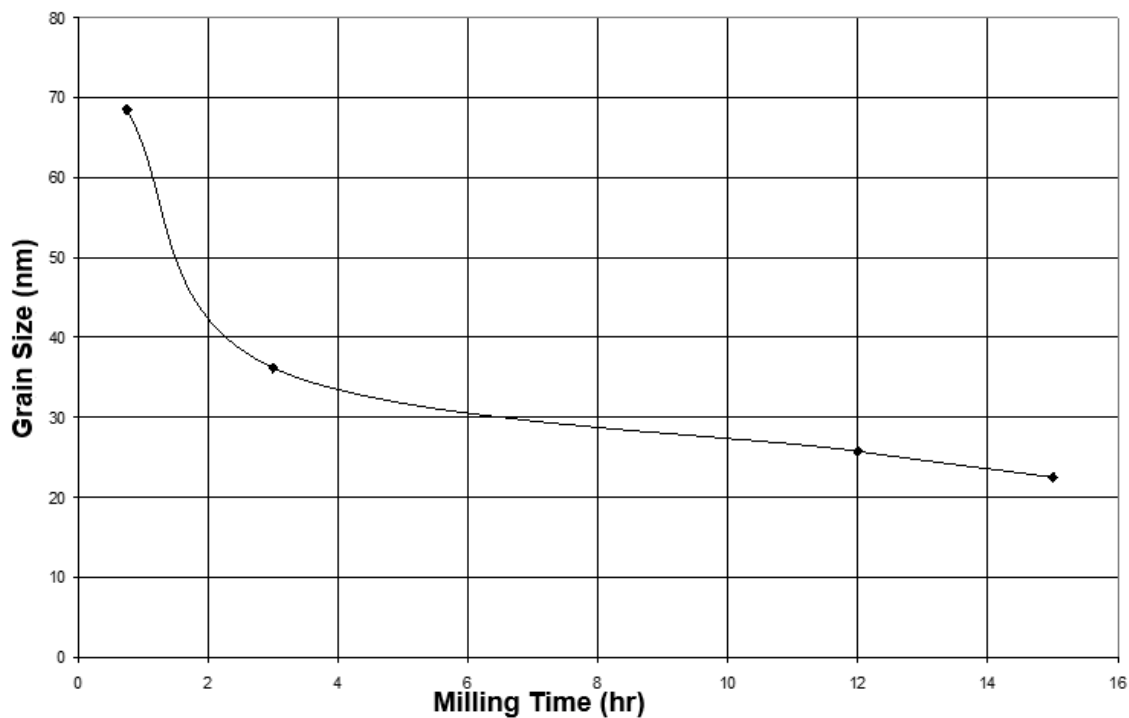


Fig. 3. Changes rate of Al6061 alloy grains size per milling time after annealing.

The MA process is a process in which the powder is always broken down and re-welded during the cold welding operation. In the next steps, with increasing milling time, these breaking-downs or fining of particles would increase and overcome the cold welding so that

the particle size reduction will continue to several tens of nanometers [19-20]. In the graph of Fig. 3, the reduction rate of grains size in the early hours of grinding has been fast between 1 to 3 hrs, while by continuing the operation, it has been observed up to 15 hrs very slow or even

without any changes. Perhaps, the reason for this rapid decline is the presence of PCA inside the mill. PCA usually decreases the cold welding between the particles, and due to collisions of balls with the powder and occurrence of work hardening, this reduction in the grains size will increase.

3-2- Examining the heated extrusion parts

3-2-1- XRD Analysis

The MA-Al-6061 / 1.25TiB₂ composite sample was tested by XRD to determine the grain size. Fig. 4 shows the XRD test results on this sample. By examining and identifying the phases, in addition to aluminum, the Al phase was also detected in the composite. Through calculating

the grain size by using sheerer equation, the size of aluminum alloy grain was measured as 95 nm. According to the data of grain size in the powders XRD experiment in Figs. 2 and 3 as well as similar results on the extruded alloy grain size (Fig. 4), it seems that the grains size has increased about 20 to 30 nm. This could be due to the extrusion temperature. For powder samples have been heated up to, a temperature of 460 °C, and then, the extrusion operation has been made. The grains growth may have occurred during the heating treatment. Such a behavior has been also observed in the case of Al-0.13Mg system [21], but the nano-structure still exists in the extruded parts.

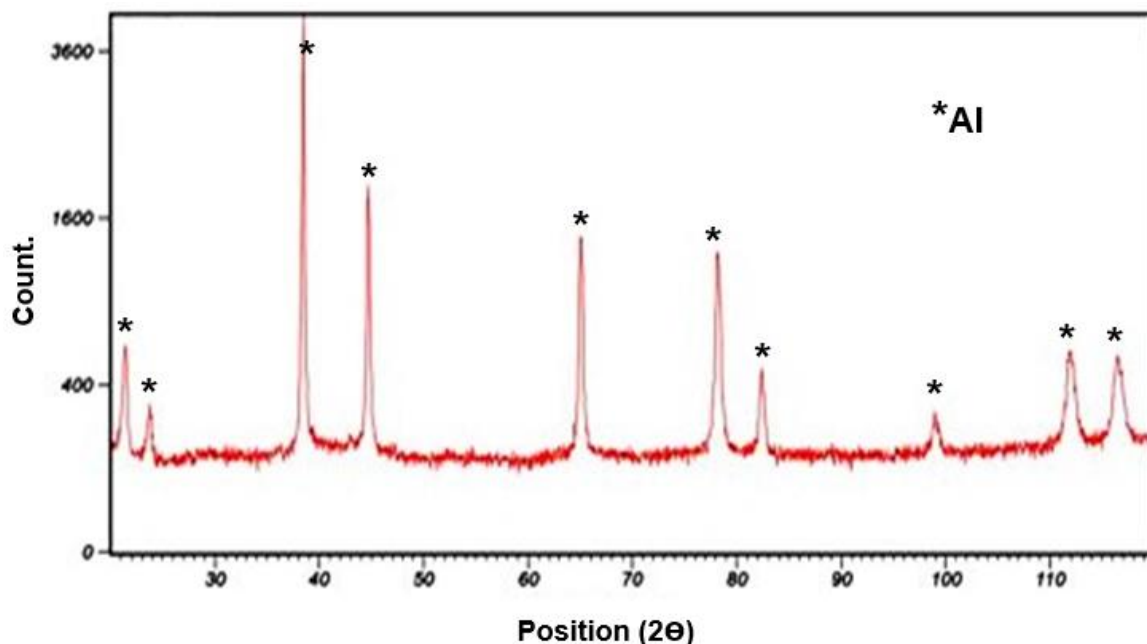


Fig. 4. XRD test results on the extruded MA-Al-6061 / 1.25TiB₂ composite alloy.

3-3- Analysis of corrosion

The corrosion rates of MA6061 and MA-Al-6061/TiB₂ samples have been shown in Fig.5 by using polarization test and drawing their relevant Tafel diagrams. The corrosion rates have been calculated using the following equation as well as Icorr software.

$$C.R. = \frac{3.27 \times 10^{-5} \times I_{corr} \times E.W}{D}$$

Where, C.R: Corrosion rate in mpy, D: Density of the corrosion sample in terms of g/cm³, EW: Equivalent weight of the corrosion sample in g/Amp.Sec, I_{corr}: Density of the corrosion

current in terms of μm /cm². Given that the density of the alloy and its equivalent weight (E.W.) are respectively as 2.6778 g/ Cm³ and 2.3821 g/Amp.Sec, the corrosion rates of the alloys tested are presented in Table 5 after calculating.

According to the results presented in Table 5 and Fig. 5, the corrosion rate of MA-Al-6061/TiB₂ composite is less than MA-Al6061 alloy. Accurately examining the corrosion behavior of this composite alloy by using XRD device studies, the composite was found to have nanostructure, while the size of MA-Al6061 alloys grains is larger than nanoscale. The nano-

structured materials have higher defects density than the polycrystalline materials. Considering that the aluminum penetration rate from the grain boundaries is high, it is likely that the pesos layer in the nano-aluminum alloy provides a better protection than the polycrystalline aluminum alloy. This case especially occurs in environments with weak alkalinity and acidity properties. A similar behavior has been seen in investigating the corrosion of Al-% 8 Fe nano-alloy [22]. It should be noted that generally the corrosion rate of composites is higher than their alloy corrosion due to galvanic corrosion between the matrix and the reinforcing phase [14-16]. However, the nanostructured nature of the studied composite has affected this effect. Such a behavior has also been observed in the study of nanostructured materials in similar studies [22-23]. The corrosion rates in two

composites of MA-Al-6061 / 1.25TiB₂ (curve 1) and MA-Al-6061 / 2.25TiB₂ (curve 2) are comparable due to identical conditions of the nanostructure and the use of MA-Al6061 powder in the manufacturing process. The only difference between the two composites is the presence of different TiB₂ percentages in these two structures. TiB₂ particles, due to their corrosion potential differences with the matrix have acted in galvanic conditions as the cathode than to the matrix (anode) that its higher percentage in the structure has increased the cathode to the anode area ratio, leading to enhanced corrosion rate [24]. Such behavior has been observed in the use of SiC particles as well. In this case, increased reinforcing particles has led to an increase in the corrosion current density [18].

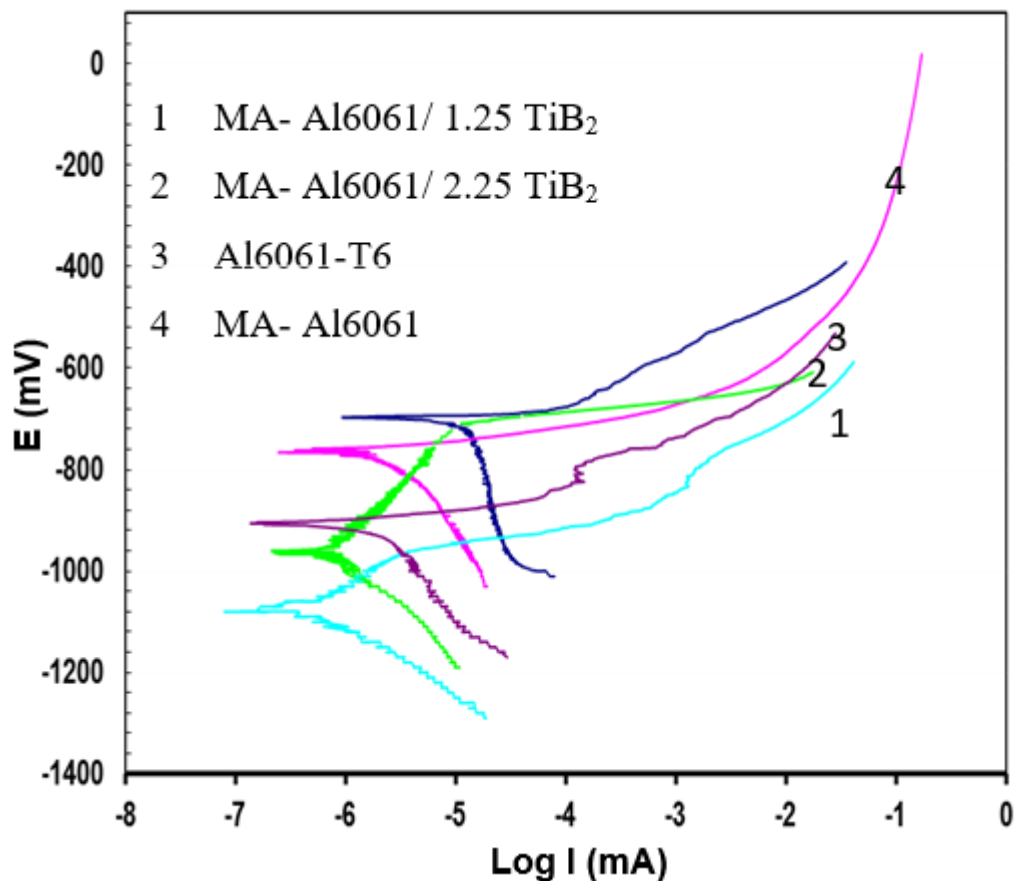


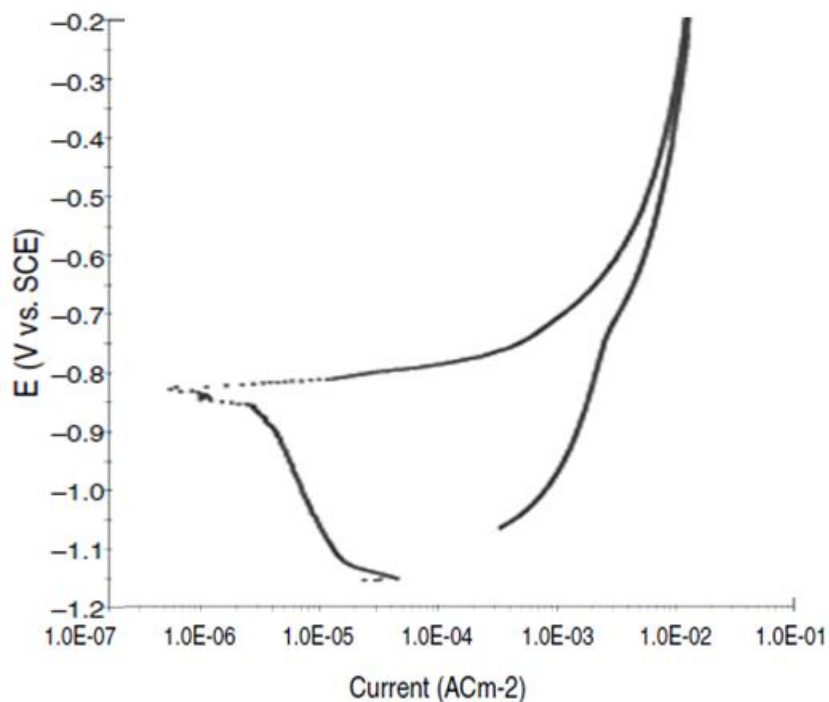
Fig. 5. Polarization test graphs of extruded nanocomposite samples.

Table 5. Corrosion rates of tested samples related to Fig. 5.

Test samples	Corrosion current ($\mu\text{m}/\text{cm}^2$)	Corrosion rate (mV)	Corrosion rate (mpy)
1 MA- Al6061/ 1.25 TiB ₂	0.253	-1080	2.805×10^{-3}
2 MA- Al6061/ 2.25 TiB ₂	1.69	-906	0.0186
3 Al6061-T6	0.686	-960	7.60×10^{-3}
4 MA- Al606	1.83	-766	0.020

Figs. 6 to 9 show the results of cyclic polarization test in the samples presented in Table 5 to evaluate the corrosion behavior of the cavities. Comparing the results of the MA-Al6061 sample's test with Al6061-T6 alloy, it can be seen that the E_{corr} has decreased in alloys made than to Al6061-T6 alloy, which has caused the passive removal and breaking down of the surface layer. This indicates the sensitization of alloy in the corrosion potential range [24]. Comparing the cyclic polarization behavior between the alloy sample and the composite

samples shown in Figs. 7 to 9 suggests the lowering of the area under the graphs loop area in the composite samples, indicating the lower sensitivity of composite samples to pitting. The presence of nanostructure in the composite samples and a high percentage of grain boundaries, in addition to reducing the sensitivity to pitting, have increased the oxidized material infiltration routes and the surface layer, and the formation of this thick layer, in the general state, has enhanced the resistance to pitting corrosion [24-25].

**Fig. 6.** Cyclic polarization graph of Al6061-T6.

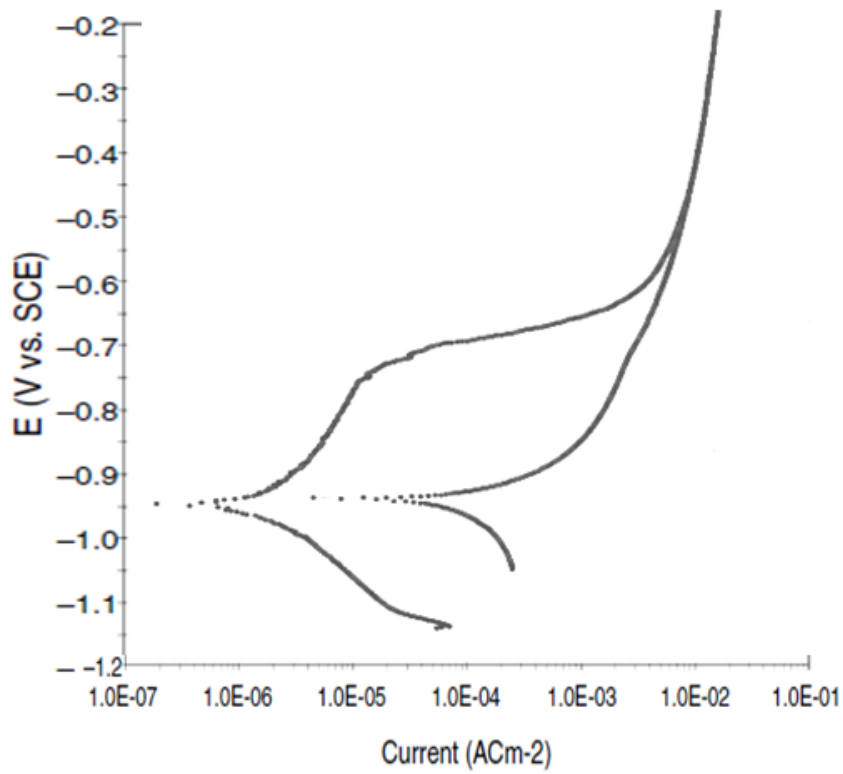


Fig. 7. Cyclic polarization graph of MA-1.

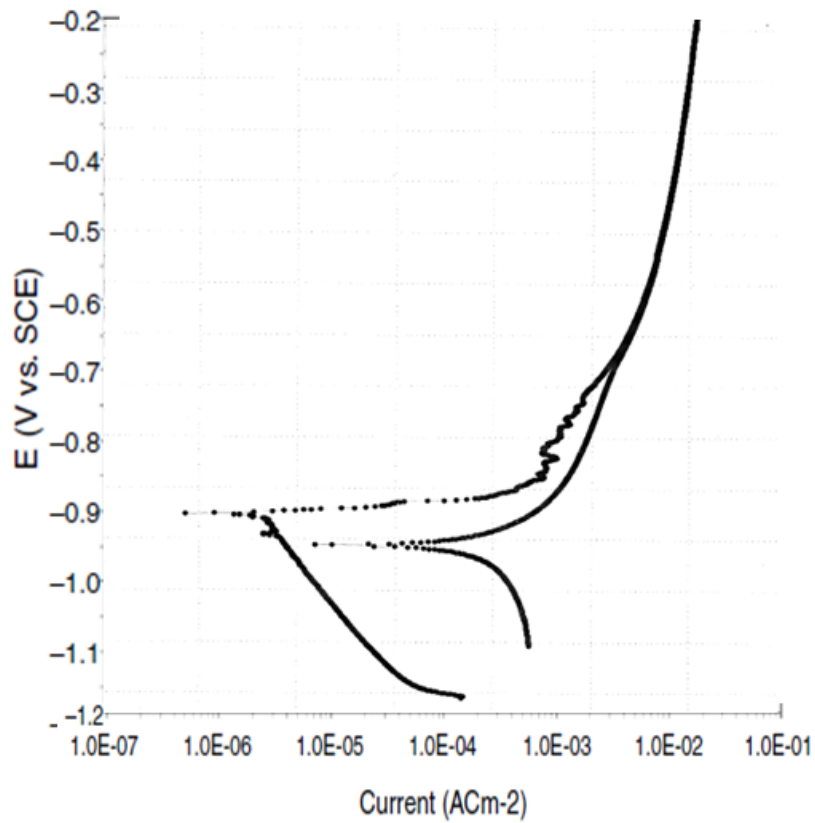


Fig. 8. Cyclic polarization graph of MA-A16061 / 1.25 TiB₂.

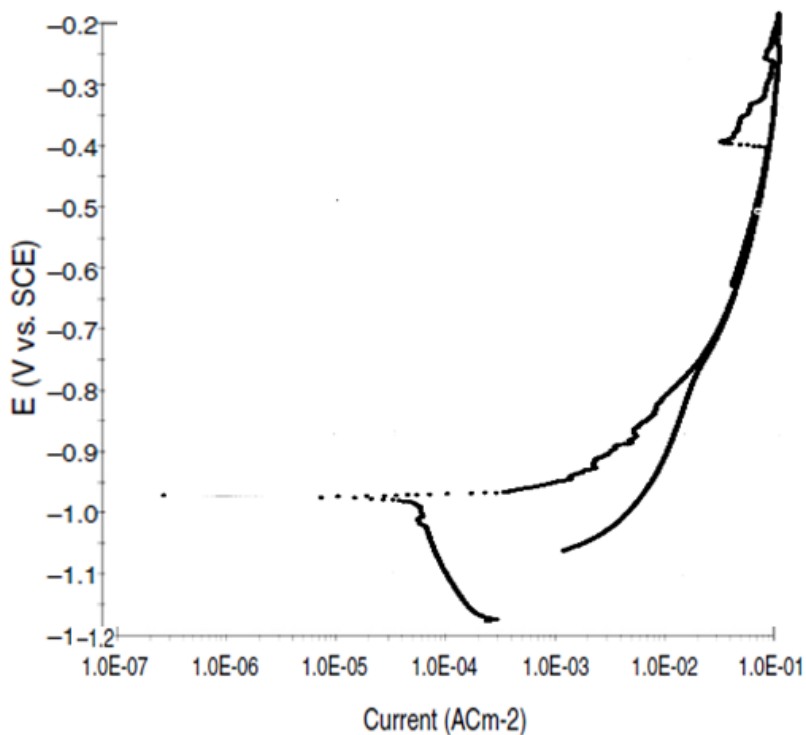


Fig. 9. Cyclic polarization graph of MA-Al-6061 / 2.25TiB₂.

4. Conclusion

1. The size of aluminum particles and its alloys in the MA process reduced to less than 4 microns and the size of its grains decreased to about 50 nm. The dispersion in the range of 20 to 70 nm can be calculated.
2. XRD analyses of the surface of heated extruded samples indicated the nanostructure nature of composite samples. Adding TiB₂ and the extruded samples at lower temperatures prevented the growth of the grains.
3. The uniform corrosion in the 2MA-Al-6061 /1.25TiB₂ composite had the lowest rate compared to other samples. The sensitivity of this alloy to pitting corrosion has raised compared to the melting state; however, this sensitivity is less than the alloy made by mechanical alloying method.

References:

- [1] N.J. Kim, Mechanical Alloying Design, Springer, 2004, p. 441.
- [2] N. Chawla and K.K. Chawla, Metal Matrix Composites, Springer, 2006, p. 1.
- [3] V.K. Lindroos, J.T. Hellman, D. Lou, R. Nowak, E. Pagounis, W. Liu, Mechanical Alloying Design, Springer, 2004, p. 667.
- [4] K.L. Tee, L. Lu, M.O. Lai, "Wear Performance of in-situ Al-TiB₂ Composites", wear, Vol. 240, 2000, pp. 59-64.
- [5] M. Narimani, B. Lotfi, Z. Sadeghian, "Investigating the microstructure and mechanical properties of Al-TiB₂ composite fabricated by Friction Stir Processing (FSP)", Mater. Sci. Eng. A, Vol. 673, 2016, pp. 436-442.
- [6] A. S. Vivekananda, S. Balasivanandha, "Wear Behaviour of in Situ Al/TiB₂ Composite: Influence of the Microstructural Instability", Tribol. Lett., Vol. 66, 2018, pp.41-56.
- [7] H. Chen, Z. Pala, T. Hussain, D.G. McCartney, "Fabrication and micro strain evolution of Al-TiB₂ composite coating by cold spray deposition", Proc. Inst. Mech. Eng., Part L: J. Mater. Des. and Appl., 2017, pp. 1-9.
- [8] G. Frommeyer, S. Knippscgeer, Aluminum-Based Metal Matrix Composites, Marcel Dekker, Vol. 2, 2003, p. 631.
- [9] J. Xu, W. Liu, "Wear Characteristic of in Situ Synthetic TiB₂ Particulate-Reinforced Al Matrix Composite Formed by Laser Cladding", J. wear, Vol. 260, 2006, pp. 486-492.

- [10] A. Kostka J. Lelatko, M. Gigla, A. Janas, "TEM Study of Interface in Ceramic-Reinforced Aluminum-Based Composites", *J. Mater. Chem. Phys.*, Vol. 81, 2003, pp. 323-325.
- [11] H.J. Sprenger, "Al Alloy/TiB₂ (Experimental Materials)", www.mmc-asses.tuwien.ac.at/data/prm/in%20situ/al-tib2.htm, 2001.
- [12] Y. Han, X. Liu, X. Bian, "Insitu TiB₂ Particulate Reinforced near Eutectic Al-Si Alloy Composites", *J. Comp. Part A*, Vol. 33, 2002, pp. 439-444.
- [13] D.W. Berkeley, H.E.M. Sallam, H. Nayeb-Hasheni, "The Effect of pH on The Mechanism of Corrosion and Stress Corrosion and Degradation of Mechanical Properties of AA6061 and Nextel 440 Fiber-Reinforced AA6061 Composite" *Corr. Sci.*, Vol. 40, 1998, pp. 141.-153.
- [14] J.B. Fogagnolo, E.M. Ruiz-Navas, M.H. Robert, J.M. Torralba, "6061 Al Reinforced with Silicon Nitride Particles Processed by Mechanical Milling" *Scrip. Materi*, Vol. 47, 2002, pp. 243-248.
- [15] M.E. Smagorinski, P.G. Tsantrizos, S. Grenier, A. Cvasin, T. Brzezinski, G. Kim, "The Properties and Microstructure of Al-based Composites Reinforced with Ceramic Particles" *Mater. Sci. Eng. A*, Vol. 244, 1998, pp. 86-90.
- [16] C. Monticelli, F. Zucchi, G. Brunoro, G. Trabanelli, "Stress Corrosion Cracking Behaviour of some Aluminum-Based Metal Matrix Composites", *Corr. Sci.*, Vol. 39, 1997, pp. 1949-1963.
- [17] J.B. Fogagnolo, F. Velasco, M.H. Robert, J.M. Torralba, "Effect of Mechanical Alloying of the Morphology, Microstructure and Properties of Aluminum Matrix Composite Powders", *J. Mater. Sci. Eng. A*, Vol. 342, 2003, pp. 131-143.
- [18] L. H. Hihara, "Corrosion of Aluminum-Matrix Composite," Ph.D. Thesis, Massachusetts Institute of Technology, 1989.
- [19] C. Suryanarayana, "Mechanical Alloying and Milling", *J. Prog. Mater. Sci.*, Vol. 46, 2001, pp. 1-40.
- [20] L. Shaw, M. Zawrah, "Effect of Process Control Agents on Mechanical Alloying of Nanostructured Aluminum alloys", *Metal. Trans. A*, Vol 34A, 2003, pp.159-170.
- [21] P.J. Apps, J.R. Bowen, P.B. Prangnel, "The effect of Second-Phase particles on the Sever Deformation of Aluminum Alloys during Equal Channel Angular Extrusion", *Proc. Nanomat. by Sev. Plas. Defo.*, 28 Jan 2005, pp.135.
- [22] W. Zeiger, M. Schneider, D. Scharnwber, and H. Worch, "Corrosion behavior of a nanocrystalline FeAl₁₈ alloy", *Nanostru. Of Mat.*, Vol. 6, 1995, pp. 1013-1016.
- [23] V. S. Saji, J. Thomas, "Nanomaterials for Corrosion Control", *Current Science*, Vol. 92, 2007, pp.51-55.
- [24] G. M. Fontana, *Corr. Eng.*, 3rd ed., Mc Graw-Hill, Singapore, pp. 112.
- [25] K. Srinivasa, K. Prasad Rao, "Pitting Corrosion of Heat-treatable Aluminum alloys and Welds: A Review", *Trans. Ind. Inst. Metal.*, Vol. 57, 2004, pp. 593-610.